研 究 解 説　　UDC 533.6.011.1

SECOND-MOMENT CLOSURES FOR RECIRCULATING AND STRONGLY-SWIRLING FLOWS
——Part 2. Applications——

再循環流および強い旋回流に対する二次モーメント完結問題
——第2部：計算適用例——

Michael. A. LESCHZINER* and Toshio KOBAYASHI**
マイケル．レシュチナー・小 林 敏 雄

The first paper argued the potential advantages of using second-moment closures in preference to eddy-viscosity models in the presence of body forces brought about by fluid recirculation, swirl and buoyancy. Results are presented in this paper for four of a total of fourteen geometries. These demonstrate that significant improvements in predictive accuracy can be achieved in flows with large recirculation regions and those involving swirl. In all cases, such improvements appear to be rooted in the ability of the closures to capture the strong response of the turbulence structure to streamline curvature.

1. INTRODUCTION

Stress-closure computations have been made for the fourteen geometries shown in Fig. 1. Moreover, in a number of cases, several different flow conditions have been examined. Space constraints only permit a small selection of results for major flow features in some of the geometries to be included; more comprehensive expositions, including comparisons for individual stress components, may be found in research papers and reports[1)~9)]. In the following three sections, results are presented for four cases, one plane, (d) in Fig. 1, one axisymmetric (g) and two swirling, (l) and (m). This selection is intended to convey a more or less representative picture of the response of the models to a range of geometric and flow conditions in which streamline curvature is a dominant feature. Specifically, flow (d) is dominated by a recirculation zone occupying a large proportion of the flow domain and surrounded by a curved wall jet. In case (g), the recirculation zone is elongated and subjected to radius effects as well as a severe adverse pressure gradient. Finally, in cases (l) and (m), very severe curvature arises from a spiralling motion rather than from curvature associated with recirculation, in addition to which strong density gradients occur in the second case.

2. PLENUM CHAMBER

The flow considered here, (d) in Fig. 1, is a cavity into which a jet is injected centrally, creating a large recirculation zone which occupies a major proportion

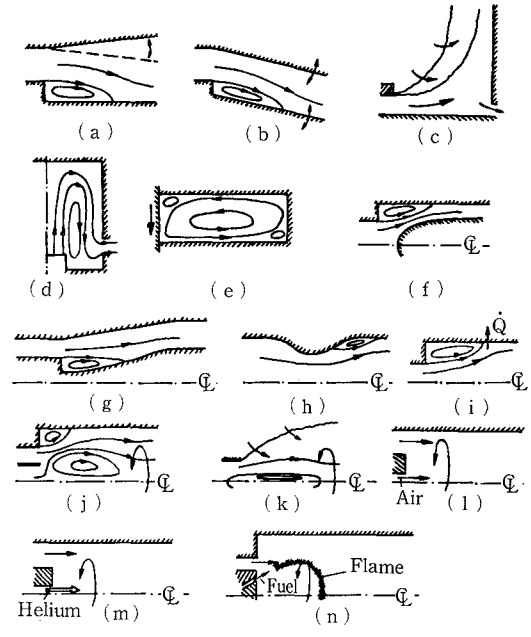

Fig. 1 Summary of flow geometries computed with second-moment closures

*Visiting Scientist (University of Manchester Institute of Science and Technology)

**Dept. of Mechnical Engineering and Navel Architecture, Institute of Industrial science, University of Tokyo

of the solution domain. Experimental LDA data for velocity and turbulence energy across the spanwise symmetry plane of the plenum have been obtained by Boyle and Golay[10]. This data must be treated with considerable caution, however, as the spanwise dimension of the chamber was too small for three-dimensional features to be assumed minor. Hence, attention must primarily focus on a comparison of performance between the models themselves rather than on accord with the experimental data. Despite this drawback, the above cavity flow has been included here in order to demonstrate that the response of the computed solution to curvature can vary dramatically, depending on the type of turbulence closure used.

Computations for this case have been made by Huang[7),11)] for grids of up to 34× 50 lines, and a representative selection of results supporting major conclusions is given in Figs. 2 to 4. First, Fig. 2 contrasts velocity-vector plots obtained with the EVM and the RSTM. It is immediately apparent that the EVM predicts a far more intense recirculatory motion in the central part of the plenum than does the RSTM. Focusing on the interaction between curvature and turbulence, it is noted that, in the inner part of the flow, the orientation of the shear strain (in a streamline-oriented co-ordinate system) relative to curvature must be expected to stabilize turbulence, thus reducing the diffusive momentum exchange between the intense shear layer adjacent to the wall and the inner region. From Fig. 3, showing velocity profiles across two lines at different plenum heights, it can be seen that both stress models predict a far thinner and steeper shear layer at the inner edge of the turning jet, which is compatible with the previous observations on the flow field. Profiles of transverse velocity at a station located at 3/4 of the chamber height, also shown in Fig. 3, reflect well the differences which may arise from using alternative models, even at mean-velocity level. The strong asymmetry in the experimental variation can be taken to indicate the existence of 3D features, in particular momentum-redistributing streamwise vorticity created by the interaction of the pressure gradient normal to the turning jet and the boundary layers on the wall confining the flow in the span-wise direction. Profiles of the average of the normal-stresses $\overline{u_1^2}$ and $\overline{u_2^2}$ are shown in Fig. 4. While a comparison with the experimental data is, as pointed out already, open to doubt, what can be observed is that the stress models yield turbulence levels by almost a factor 4 lower than the EVM. Lest the high level returned by the latter is held to be erroneous, it is noted that EVM calculations presented for this case by several groups at a recent IAHR workshop[11)] showed similar levels. It is, moreover, of some importance to point out that the ASM and RSTM calculations were obtained by two independent codes, incorporating quite different coding methodologies. The close correspondence between the two sets of predictions encourages the

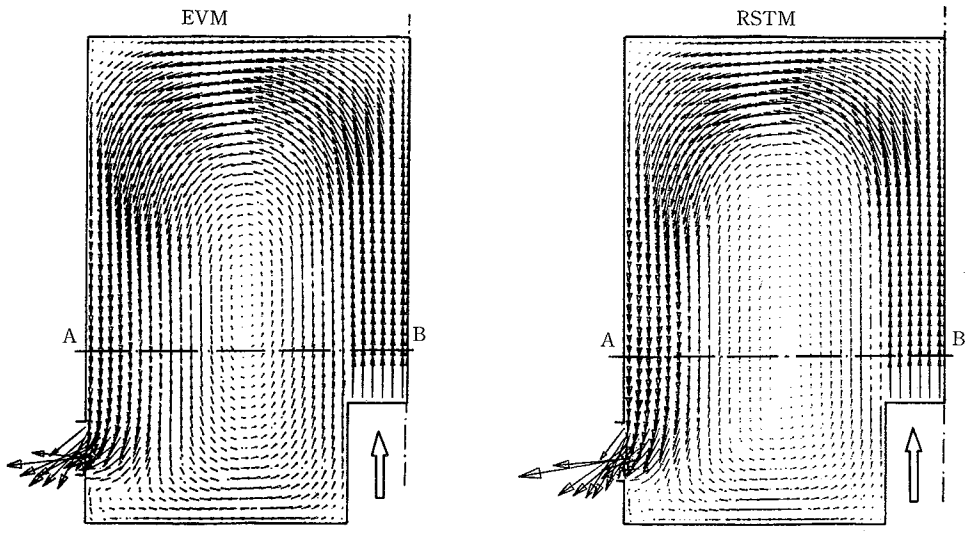

Fig. 2 Flow in plenum chamber: velocity fields computed with EVM and RSTM

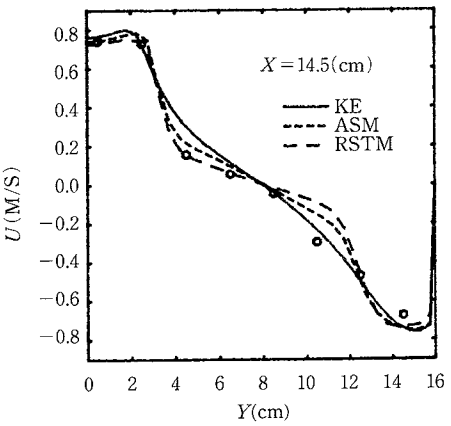

conclusion, therefore, that the behaviour shown genuinely reflects the basic capabilities of the stress closures.

3. AXI-SYMMETRIC FLOW OVER STEPPED CENTREBODY IN DIFFUSOR

The second geometry, (g) in Fig. 1, consists of a stepped and shaped centre-body suspended in a diffuser which imparts a severe adverse pressure gradient on the flow. This gradient, whose intensity may be varied by shifting the centrebody axially, tends to elongate the recirculation zone and intensify the motion therein. Experimental results for this flow have been obtained by Lea[12], and related computations have been performed by Kadja[4] with the mesh shown in Fig. 5.

A comparison between the streamfunction contours predicted for one of three centre-body positions with the EVM and ASM, both with the PLDS and QUICK approximations for convection, is shown in Fig. 6. The experimentally observed reattachment point (found with the aid of an oil-film technique) is marked on the plot, and it is seen that the ASM/QUICK-calculated separation streamline reattaches closest to this value. A certain degree of sensitivity to the numerical approximation is displayed in this case, and this suggests that grid refinement, mainly in the axial distribution, would have been desirable. It will be noted that the separation zone is unusually extensive for a back-step type flow, and this is due, of course, to the additional adverse pressure gradient imparted by the diffuser. In consequence, this case, like that considered in the previous section, represents a sensitive test of the turbulence model's ability to predict the flow accurately.

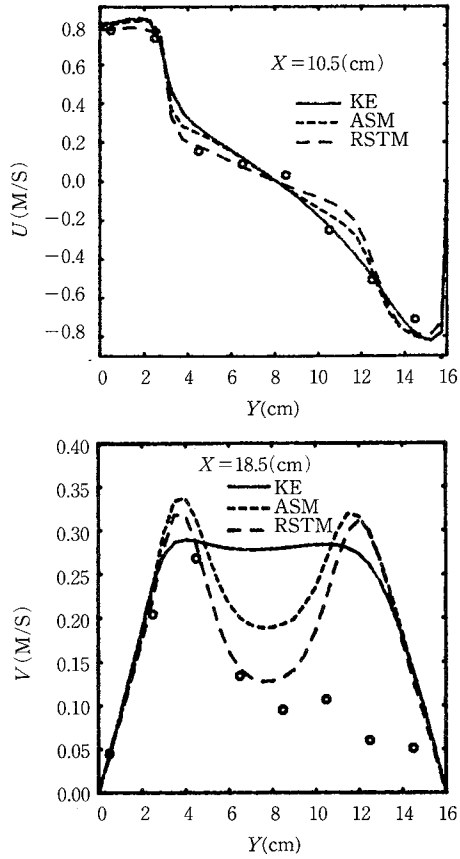

Fig. 3 Flow in plenum chamber: U- and V-velocity profiles

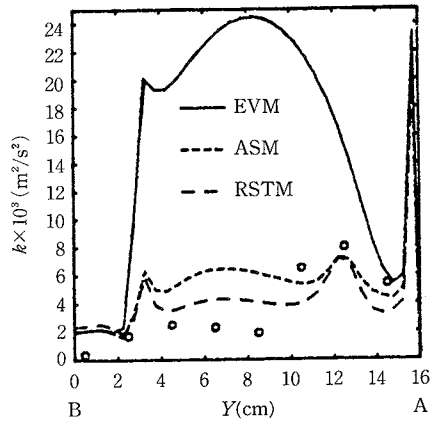

Fig. 4 Flow in plenum chamber: profiles of 0.5 $(\overline{u^2}+\overline{v^2})$

The clear superiority of the ASM over the EVM is further highlighted in Fig. 7 by predicted pressure-recovery variations, expressed via the pressure coefficient $2(P-P_0)/\rho U_{in}^2$, along the diffuser wall for two centre-body positions. The fact that the experi-

mental variations are well reproduced indicates that the outline and shape of the recirculation bubble has been well captured, for the separation streamline may be taken to mimic a solid inviscid wall whose location will govern the pressure variation in the main stream. A comparison of velocity and turbulence-intensity profiles, not included here, tends to add support to the ASM, but reveals discrepancies (with both models) in the recovery zone beyond the point of reattachement close to the diffuser wall. Far downstream, in particular, the experimental boundary-layer thickness is found to be significantly larger than the computed one, implying a greater tendency towards separation. The origin of this defect is not fully established yet, but there is some general evidence that boundary layers subjected to strong adverse pressure gradients are not well predicted with the present type of closures due to the fact that the dissipation-rate equation produces an excessive level of length scale near the wall which, in turn, results in excessive near-wall mixing and wall-shear stress.

4. STRONGLY-SWIRLING FLOWS

The application of the stress models to two swirling flows, one with strong density gradients, concludes this overview. Such flows, particularly if recirculating, are arguably not only the most complex of all 2 D configurations from a physical standpoint, but also pose special computational problems. These arise from the stiff coupling between the swirl- and radial -momentum equations, the presence of three interacting shear stresses rather than one, and the occurrence of 'sub-critical' conditions in confined flows, similar to those prevailing in sub-critical free-surface flow.

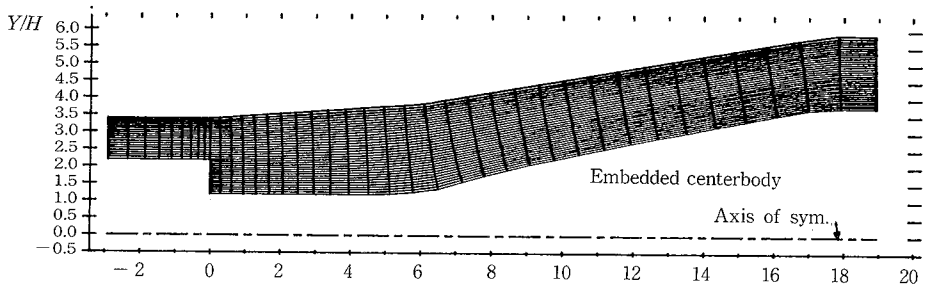

Fig. 5 Flow over stepped centre-body in diffuser: numerical mesh

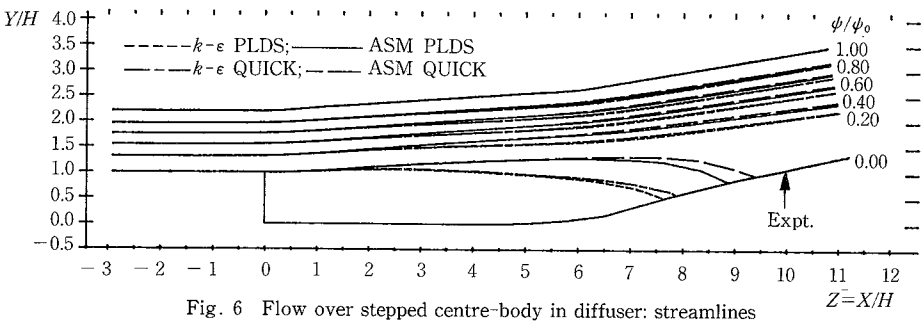

Fig. 6 Flow over stepped centre-body in diffuser: streamlines

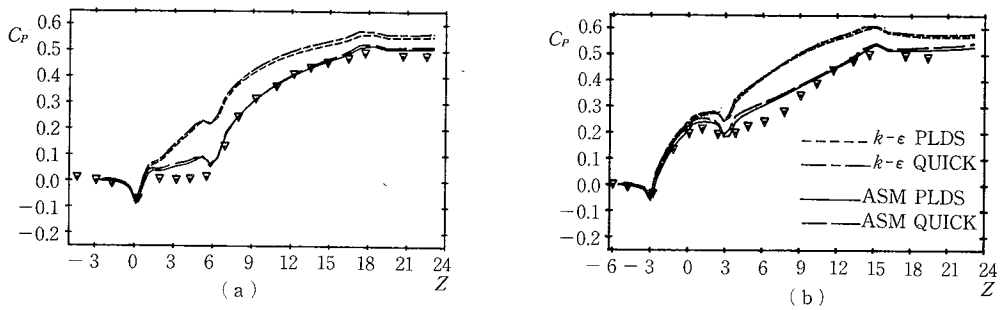

Fig. 7 Flow over stepped centre-body in diffuser: pressure coefficient on diffuser wall for two centre-body positions

The two cases chosen, (l) and (m) in Fig. 1, are virtually identical in geometric terms, both consisting of two concentric jets discharged into a smooth outer pipe, with the outer jet swirled. In case (m), however, the inner jet is made up of a mixture between helium and air, giving a density ratio at inlet of 4.3. Both configurations operate at the very high swirl number $S=2.2$. Measurements have been made by So et al[13] for case (l) and by Ahmed and So[14] for case (m). All related computations have been performed by Hogg[2),3)] with grids of upto 48×48 lines.

Before attention is directed to comparisons between experiment and prediction, is instructive to note that both flows are highly unusual, for swirl decays very slowly, with swirl profiles indicating a tendency towards solid-body-type rotation, while the stream-wise centre-line velocity diminishes continuously rather than recovers, with a trend towards reversal far downstream. In such conditions, curvature is expected to severely attenuate turbulence and to inhibit radial diffusion. This type of flow has been termed "sub-critical" by Squire[15], for it has been observed that even slight disturbances introduced far downstream propagate upstream, provoking material changes to the flow structure. It is this flow character which has here necessitated the imposition of Dirichlet boundary condition for streamwise velocity at the *outlet* as well as at the inlet when RSTM calculations were performed.

Computational results for the uniform-density case are shown in Figs. 8 to 10. The first compares predicted variations of centre-line velocity with experimental data. Focusing on model sensitivity rather than on the effect of exit conditions, it is seen that the EVM 'resists', or more accurately tends to 'ignore', the downstream constraints up to $x/D\simeq 20$, predicting a steady recovery, normally expected in 'super-critical' conditions. In contrast, the RSTM returns a steady decay in good accord with experiment. Removal of the downstream constraints in the RSTM calculation has been found to produce unrealistic reverse flow over a large portion of the right-hand-side exit plane. A comparison of the radial profiles of axial and swirl velocity in Figs. 9

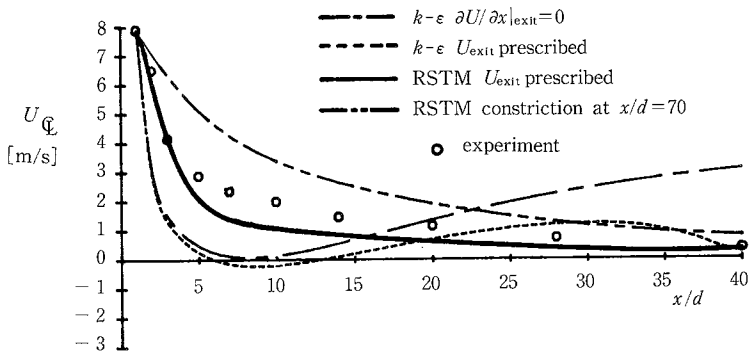

Fig. 8 Constant-density swirling flow in tube: variation of centre-line velocity

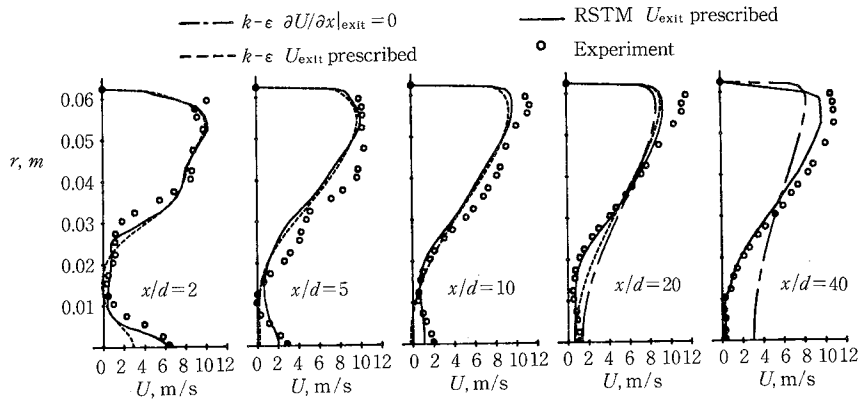

Fig. 9 Constant-density swirling flow in tube: profiles of axial velocity

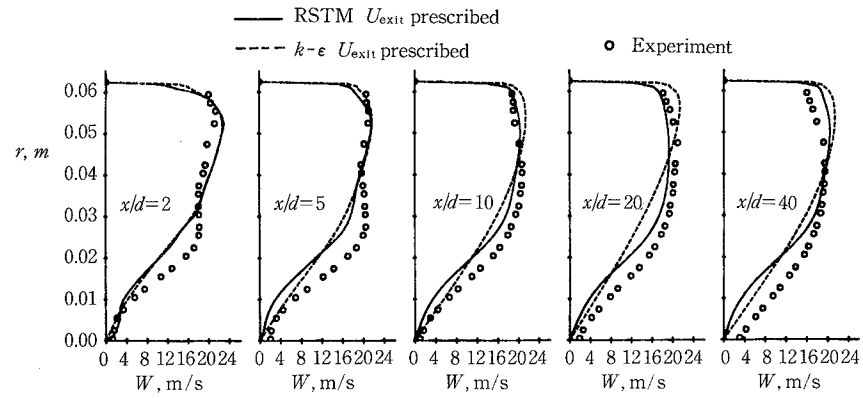

Fig. 10 Constant-density swirling flow in tube: profiles of swirl velocity

and 10, respectively, clearly shows that the k-ε model predicts excessive diffusion levels, leading to more rapid radial mixing and improper flow recovery. In contrast, the RSTM correctly mimics the depression of mixing, maintaining the sub-critical nature of the flow.

Sample results for the variable-density case, obtained with two slightly different versions of a density-weighted stress/flux-transport closure, are shown in Figs. 11 to 14. A particularly curious feature of this flow, seen in Fig. 11, is that the central (helium/air) jet retains its integrity to a far greater extent than in the previous constant-density case, although, here, the momentum of the jet is much lower. This behaviour may primarily be attributed to swirl-induced centripetal acceleration 'confining' the low-density jet fluid to the inner radial region. Swirl, aided by the positive density gradient, produces a severe attenuation of the shear-stress field, and the inner jet is partially 'decoupled' from the outer flow with very little radial mixing taking place. The profiles of swirl velocity and circumferen-

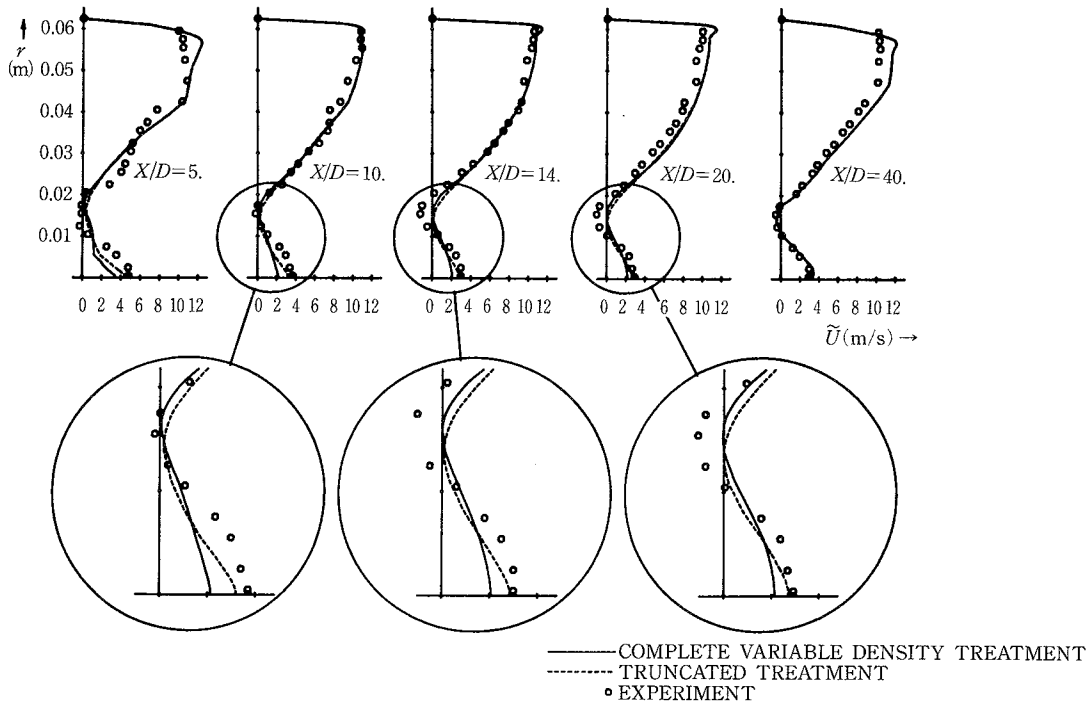

Fig. 11 Variable-density swirling flow in tube: profiles of axial velocity

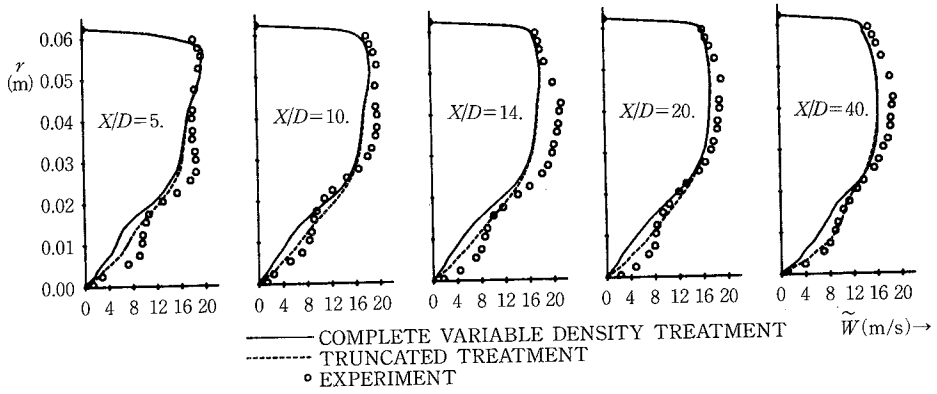

Fig. 12 Variable-density swirling flow in tube: profiles of swirl velocity

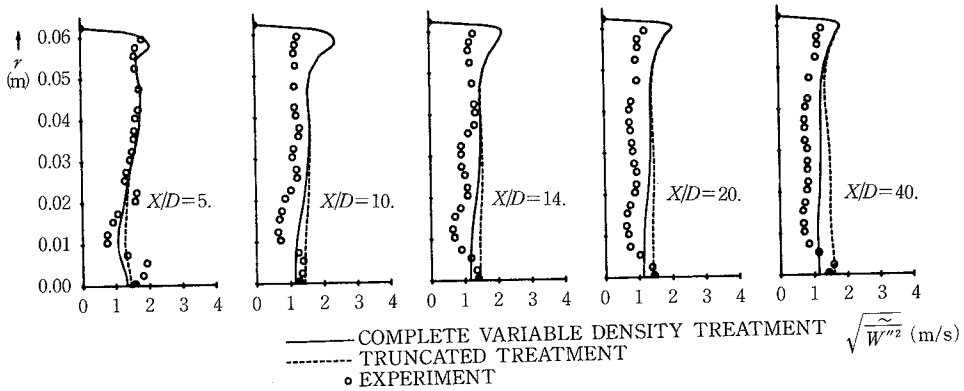

Fig. 13 Variable-density swirling flow in tube: profiles of circumferential turbulence intensity

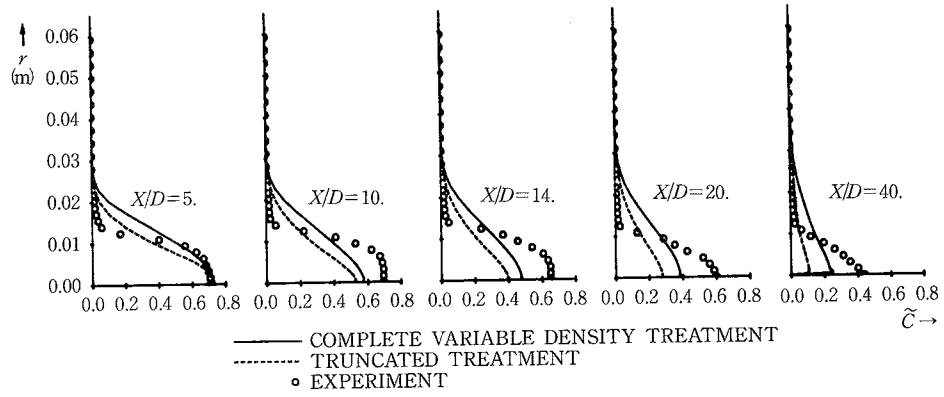

Fig. 14 Variable-density swirling flow in tube: profiles of centre-jet mixture fraction

tial turbulence intensity shown in Figs. 12 and 13, respectively, lend further support to the assertion that the stress model captures well the aerodynamic behaviour. A less satisfactory degree of agreement is obtained, however, in respect of the jet's scalar mixture fraction. As seen from Fig. 14, radial diffusion is still excessive, even though the stress model is found to predicts very low levels of shear and radial flux. This result is one of a number taken to indicate that specifically the model of pressure/scalar-gradient interaction in the flux equations requires re-examination and improvement; this is an area of current research.

5. CONCLUDING COMMENTS

An outline has been provided of recent progress

made in computing complex recirculating and strongly swirling flows with Reynolds-stress closures and non-diffusive discretization within the finite-volume framework.

In the case of plane flows, stress closures have generally been found to be especially appropriate and beneficial when the flow is dominated by a recirculation zone 'driven' by a shear layer in which curvature attenuates turbulent transport, particularly if this shear layer is adjacent to a wall. In swirling flows, the identification of defects in the algebraic representation of stress transport have led to the exclusive use of full stress closures. Studies focusing on other axisymmetric flow, not reported here, indicate that this conclusion applies more generally. With the algebraic model excluded, swirling flows draw particular benefits from stress closure in situations in which curvature attenuates turbulence within a shear region bordering a wall; this conclusion has been found to apply to both constant- and variable-density conditions.

While stress closures bring about notable improvements in predictive accuracy, differences between calculations and measurements are not always reduced to insignificant levels, indicating that model defects remain. The models of pressure- strain interaction and stress diffusion undoubtedly contribute to these defects. Probably, a more important source of errors is the representation of dissipation by a single isotropic parameter which is, in addition, insensitive to stress anisotropy.

ACKNOWLEDGEMENT

Different parts of the work have been supported by the UK Science and Engineering Research Council, Rolls Royce plc, The UK Department of Trade and Industry, British Aerospace, Nielson Engineering and Research Inc. and The Foundation for the Promotion of Industrial Science.

(Manuscript received, April 1, 1988)

REFERENCES

1) Leschziner M A, - Numerical implementation and performance of Reynolds-stress closures in finite -volume computation of recirculating and strongly swirling flows, Report TFD/87/8, UMIST, Dept Mech Eng, Thermofluids Div, 1987. Also, lecture notes in Introduction to the Modelling of Turbulence, von Karman Institute, Brussels, May 1987.

2) Hogg S and Leschziner M A, - Computation of highly swirling confined flow with a Reynolds -stress turbulence model, Report TFD/86/12, UMIST, Dept Mech Eng, Thermofluids Div, 1986. (Accepted for publicationn in J AIAA, 1987).

3) Hogg S and Leschziner M A, - Second-moment -closure calculation of strongly swirling confined flow with large density gradients, Report TFD/87/10, UMIST, Dept Mech Eng, Thermofluids Div, 1987. (Submitted to Int J Heat Fluid Flow, 1987).

4) Kadja M, - Computation of recirculating flow in complex domains with algebraic Reynolds-stress closure and body-fitted meshes, Ph.D. Thesis, University of Manchester, 1987.

5) Huang P G and Leschziner M A, - Stabilization of recirculating flow computations performed with second-moment closure and third-order discretization, Proc 5th Symp on Turbulent Shear Flows, Cornell University, p 20.7, 1985.

6) Fu S, Launder B E and Leschziner M A, - Modelling strongly swirling recirculating flow with Reynolds stress transport closures, Proc 6th Symp on Turbulent Shear Flows, Toulouse, p 17.6, 1987.

7) Huang P G, - The computation of elliptic turbulent flows with second moment closure models, PhD thesis, University of Manchester, 1986.

8) Fu S, Huang P G, Launder B E, Leschziner M A, - A comparison of algebraic and differential second-moment closures for axisymmetric turbulent shear flows with and without swirl, Report TFD/86/9, UMIST, Dept Mech Eng, Thermofluids Div, 1986. (Accepted for publication in ASME J Fluids Eng, 1987).

9) Leschziner M A, - Finite-volume computation of recirculating flow with Reynolds-stress turbulence closures, Proc 3rd Int Conf on Numerical Methods for Non-Linear, Problems, Dubrovnik, p 847, 1986.

10) Boyle D R and Golay M W, - Measurement of a recirculating two-dimensional flow and comparison to turbulence model prediction. I: Steady state case, J Fluids Eng, Vol 105, p 446, 1983.

11) Grandotto M, - First comparisons of contributed computations, 9th IAHR Workshop on Refined Modelling of Flows, Marseilles, 1985.

12) Lea C J - Hot-wire measurements of turbulent flow over a sudden centrebody contraction placed in a diffusor, MSc Thesis, University of Manchester, 1987.

13) So R M C, Ahmed S A and Mongia H C, - An experimental investigation of gas jets in confined swirling air flow, NASA CR-3832, 1984.

14) Ahmed S A and So R M C, - Concentration distribution in a model combustor, Expt. in Fluids, Vol 4, p 107, 1986.

15) Squire H B, - Analysis of the vortex breakdown phenomenon, Miszellanen der Angewandten Mechanik, Akademie, Berlin, p 306, 1962.